Desalination and Water Treatment
www.deswater.com
doi: 10.1080/19443994.2015.1077747

57 (2016) 16119–16128
July

Taylor & Francis
Taylor & Francis Group

Mineralization of unsymmetrical dimethylhydrazine (UDMH) via persulfate activated by zero valent iron nano particles: modeling, optimization and cost estimation

Ali Reza Zarei[a,*], Hadi Rezaeivahidian[a], Ali Reza Soleymani[b]

[a]*Department of Chemistry and Chemical Engineering, Malek Ashtar University of Technology, Tehran, Iran, Tel./Fax: +98 21 22938641; emails: zarei128@gmail.com (A.R. Zarei), hrvahidian_1984@yahoo.com (H. Rezaeivahidian)*
[b]*Faculty of Science, Department of Applied Chemistry, Malayer University, Malayer 65719, Iran, Tel. +98 851 3339843; email: a.r.soleymani@malayeru.ac.ir*

Received 21 February 2015; Accepted 22 July 2015

ABSTRACT

This work examined the mineralization of unsymmetrical dimethylhydrazine (UDMH) as an alarming organic contaminant, via persulfate (PS) oxidation process. Nano zero-valent iron (NZVI) particles, as a source of ferrous ions, were synthesized and used to activate PS ions in the media. The effective operational parameters such as NZVI dosage, pH, and initial amount of PS were optimized by response surface methodology as a statistical experimental design. The mineralization efficiency and the demand-operating cost (DOC) of the process were well modeled by two second-order polynomial equations. Based on the desirability, function optimization of the responses was performed. In the optimum condition of pH 3.45, $[PS]_0$ = 836.16 mg L^{-1}, and $[NZVI]_0$ = 158.45 mg L^{-1}, the model predicted 91% of the UDMH mineralization and 10 US$/$m^3$ for the DOC that the electrical energy constitutes 69% of the total cost. Compared with the related literatures about treatment of the UDMH, the applied NZVI/PS process reached a high efficiency using lower chemicals.

Keywords: Dimethyl hydrazine; Stabilized nano zero-valent iron; Persulfate oxidation; UDMH mineralization; Cost estimation

1. Introduction

Unsymmetrical dimethylhydrazine (UDMH) is a derivative of hydrazine and is volatile such that it is readily absorbed by dermis [1]. The UDMH has been classified in group B2 (human carcinogen) based on sufficient evidence of carcinogenicity from studies in animals [2]. UDMH is miscible in water and will migrate into water sources and can be dangerous for water consumers. The LD_{50} of the UDMH in rats is 104 mg kg^{-1} which suggests that UDMH has a high toxicity [3]. UDMH is an explosive, which is mainly used as a liquid propellant in military applications. Because of higher stability of UDMH rather than hydrazine, especially at elevated temperatures, it can be used as hydrazine replacement [4]. Local pollution with UDMH may be reached in tonnes, whereas trace amounts of UDMH and its incomplete oxidation products may retain in soil even more than 10 years [5].

Advanced oxidation processes (AOP) are *in situ* techniques which able to mineralize organic hazardous material by highly active radicals (i.e. hydroxyl

*Corresponding author.

and sulfate radicals) [6,7]. For mineralization of hazardous organic materials such as pesticides, azo dyes, trinitrotoluene, and dimethylhydrazine, AOPs are preferred rather than physical and biological methods [8–11]. The mineralization process means complete oxidative degradation of an organic matter to the carbon dioxide and water. Success in the mineralization of a hazardous pollutant is important, since remaining stable intermediate in the media may possess poisonous.

Recently, application of indirect oxidation via activated persulfate (PS) ions is one of the promising AOP methods [6,12]. PS ion with oxidation potential of 2.01 volt can produce more oxidative sulfate radical (oxidation potential of 2.6 volt) via thermolysis, photolysis, or chemical activation by transition metals as shown in Eqs. (1) and (2). In the aqueous media, the sulfate radicals can generate hydroxyl radicals (Eq. (3)) and the radicals can initiate a series of chain oxidation reactions which are led to the mineralization of organic pollutants in water (Eq. (4)) [13–15].

$$S_2O_{8(aq)}^{2-} \xrightarrow{heat/h\upsilon} 2SO_{4(aq)}^{\bullet -} \tag{1}$$

$$S_2O_{8(aq)}^{2-} + M_{(aq)}^{n+} \rightarrow SO_{4(aq)}^{2-} + SO_{4(aq)}^{\bullet -} + M_{(aq)}^{(n+1)+} \tag{2}$$

$$SO_{4(aq)}^{\bullet -} + H_2O_{(l)} \rightarrow SO_{4(aq)}^{2-} + HO_{(aq)}^{\bullet} + H_{(aq)}^{+} \tag{3}$$

$$SO_{4(aq)}^{\bullet -} + HO_{(aq)}^{\bullet} + \text{organic pollutant} \rightarrow \text{intermediate} \rightarrow CO_{2(g)} \tag{4}$$

Because of the good efficiency of the chemical method at ambient temperature [16], and also the high cost of heat and light providing when a high amount of effluent is to be handled, the chemical activation method is more attractive.

In chemical activation method, transition metal ions such as Fe(II), Cu(I), and Ag(I) have been used [14,17]and in that iron is more attractive due to its non-toxicity and low cost. Eq. (5) shows that the sulfate radical is produced by PS and Fe^{2+} interaction with rate constant of 2×10^1 ($M^{-1}s^{-1}$). On the other hand, the ferrous ions can quench the sulfate radicals with rate constant of 4.6×10^9 ($M^{-1}s^{-1}$) (Eq. (6)) [18]. Therefore, quenching of sulfate radical is intensively occurred in the presence of excess ferrous iron ions.

$$S_2O_{8(aq)}^{2-} + Fe_{(aq)}^{2+} \rightarrow SO_{4(aq)}^{2-} + SO_{4(aq)}^{\bullet -} + Fe_{(aq)}^{3+} \quad k = 2 \times 10^1 (M^{-1}s^{-1}) \tag{5}$$

$$SO_{4(aq)}^{\bullet -} + Fe_{(aq)}^{2+} \rightarrow SO_{4(aq)}^{2-} + Fe_{(aq)}^{3+} \quad k = 4.6 \times 10^9 (M^{-1}s^{-1}) \tag{6}$$

In order to reduce the quenching process, the ferrous ion dosage in the reaction media should be kept low during the chemical-activated PS process. To this aim, application of nano zero-valent iron (NZVI) particles as a source of Fe^{2+} ions has been suggested (Eqs. (7)–(9)) [19].

$$S_2O_{8(aq)}^{2-} + Fe_{(s)}^{0} \rightarrow 2SO_{4(aq)}^{2-} + Fe_{(aq)}^{2+} \tag{7}$$

$$\frac{1}{2}O_{2(aq)} + Fe_{(s)}^{0} + H_2O_{(l)} \rightarrow 2OH_{(aq)}^{-} + Fe_{(aq)}^{2+} \tag{8}$$

$$2H_{(aq)}^{+} + Fe_{(s)}^{0} \rightarrow H_{2(g)} + Fe_{(aq)}^{2+} \tag{9}$$

As the Eq. (5) shows to activate PS ion, Fe^{2+} ion is converted to the Fe^{3+}, that in the presence of NZVI particles, the ferrous ion can be recycled and reused through the following reaction [20].

$$2Fe_{(aq)}^{3+} + Fe_{(S)}^{0} \rightarrow 3Fe_{(aq)}^{2+} \tag{10}$$

The NZVI particles possess higher surface area than the microparticles, but some problems which accompany with NZVI particles are their rapid oxidation and agglomeration, which make their storage difficult and can be an impediment to the application of them. As a solution, the NZVI particles are often covered with hydrophobic stabilizers such as carboxy methyl cellulose (CMC) and chitosan [21,22].

In the present study, the chemical-activated PS as an AOP method is studied to mineralize UDMH as a typical hazardous matter in the aqueous media. Activation of PS ions is performed using NZVI particles as a source of ferrous ion. The particles were prepared via chemical precipitation method and were well stabilized by encapsulation with starch molecules as an eco-friendly stabilizer. The response surface methodology (RSM) as a statistical experimental design is applied to model the process based on the operational factors such as the NZVI dosage, pH, and initial amount of the PS. The process is optimized considering both the efficiency and the demand-operating cost (DOC). A comparative review is done between this research and existance literatures about oxidation removal of UDMH.

2. Experimental

2.1. Reagents and apparatus

All chemicals and reagents were in analytical grade. UDMH ($C_2H_8N_2$ and $M_w = 60.10$ g mol^{-1}) and sodium borohydride were purchased from Fluka. Sulfuric acid, sodium hydroxide, potassium PS, starch, and ferrous sulfate were Merck products. In all of the experiments, deionized water was used to prepare the solutions. Measurement of the pH was done by a pH meter (PH.Z.S.PTR79) and the reaction samples were mixed by a shaker (heidolph DSC304, 30 W). Total organic carbon (TOC) analysis was performed using a multi N/C 3100 (Germany) instrument. The size of NZVI particles was evaluated by transmission electron microscopy (TEM) (H-800, Hitachi, Japan) and dynamic light scattering (DLS) (PSS, Malvern, CA).

2.2. Synthesis of NZVI particles and its characterization

Chemical precipitation method was applied to synthesize the NZVI particles. Firstly, in order to prepare the solutions, 500 ml of deionized water was deoxygenated by nitrogen gas. Then 10 ml of $FeSO_4$ solution (0.2 mol L^{-1}) and 10 ml of starch solution (as a modifier, 1% w/w) were poured into a 250-ml flask and well mixed by mechanical stirrer. The mixture was purged with nitrogen gas for half an hour to remove remained dissolved oxygen. Then, the solution was slowly titrated using 10 ml of $NaBH_4$ (1.0 mol L^{-1}) to reduce the Fe(II) ions to NZVI (Eq. (11)). Excess $NaBH_4$ was added to accelerate and complete the precipitation and for the uniform growth of the iron nanoparticles [23,24].

$$Fe^{2+}_{(aq)} + 2BH^{-}_{4(aq)} + 6H_2O_{(l)} \rightarrow Fe^{0}_{(s)} + 2B(OH)_3 + 7H_{2(g)} \quad (11)$$

TEM image of synthesized NZVI particles and its histogram are demonstrated in the Fig. 1. The figure reveals that the size distribution of the synthesized NZVI particles is widespread in the range of 20–60 nm (mean diameter of 40 nm). Also, size distribution of the nanoparticles is shown in Fig. 2. The spectrum shows two peaks which the peak at 103 nm is correlated with 67.6% of the synthesized particles, and shows covering of the NZVI particles by the starch molecules. The second peak at 650 nm is related to 32.4% of the particles which are non-dissolved starch particles. Comparison of TEM and DLS results confirm the encapsulation of NZVI particles by the starch molecules.

2.3. Procedure and sample analysis

In all the experiments, initial dosage of UDMH molecules was 50 mg L^{-1} in the solutions. For each test, a desired amount of NZVI particle suspension was sonicated and poured into an Erlenmeyer flask and then the particles were separated from the solvent via magnetic decantation. Before each run to remove the starch layer, the NZVI particles were rinsed using ethanol and water. Then, 50 ml of the UDMH solution was added to the NZVI particles in a flask and pH of the suspension was adjusted at a desired value. Then a certain amount of the PS was added and the shaker was switched on for well mixing. Sampling was done after 40 min, then the remained NZVI particles were separated by a magnet and the sample was analyzed using a TOC meter to assess the extent of mineralization. It is notable that, in order to quench the oxidative radicals after sampling, a known amount of sodium sulfite was added into the solution. It is well known that in the presence of ferric and ferrous ions, especially at the basic pHs, coagulation of pollutants is occurred [25]. Therefore, to avoid any defect in the accuracy of the TOC assessment, all samples were acidified (pH 2) before the analysis.

2.4. The efficiency and operating cost of the process

The efficiency of the treatment process (X) was defined based on the extent of the mineralization of UDMH molecules under different conditions as:

$$X = \frac{TOC_0 - TOC_t}{TOC_0} \quad (12)$$

where TOC_0 and TOC_t are the initial and final (after 40 min of the process) TOC of the experimental samples, respectively.

The DOC of the process has a vital importance in the economical and applied point of views. In this work, the DOC of the NZVI/PS process was estimated based on the total price of the used chemicals (Table 1) and electrical energy consumed at the process under various conditions. For each process, the electrical energy cost (EEC) can be calculated as:

$$EEC = \frac{P \times t \times S}{V \times X} \quad (13)$$

where EEC is the electrical energy cost (in US\$/m^3), P is the consumed electrical power by the applied shaker (in kWh), t is the time of the process (in h), S is the

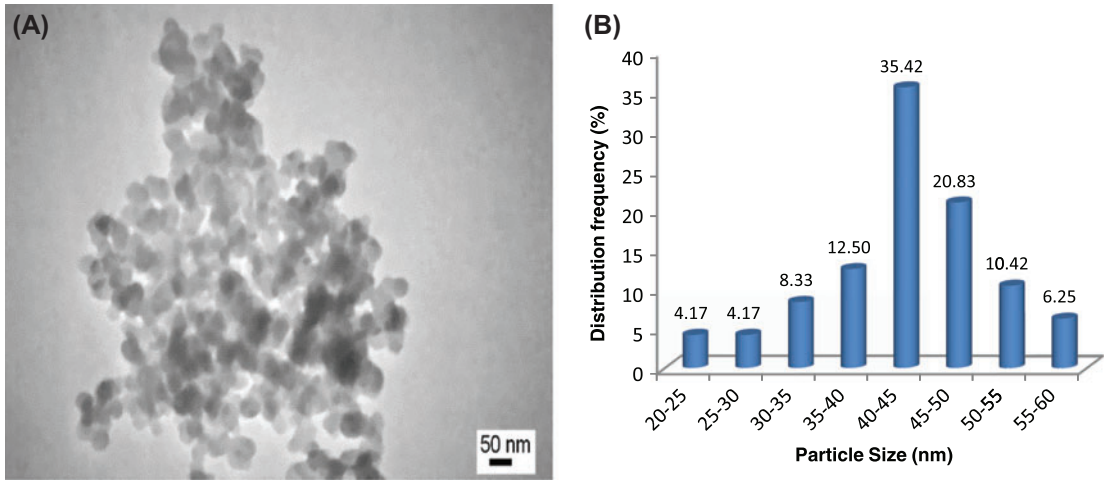

Fig. 1. (A) TEM image of the stabilized NZVI particles and (B) distribution of the particle size.

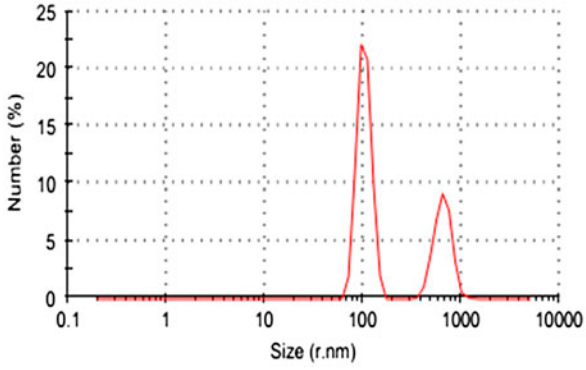

Fig. 2. DLS graph of the stabilized NZVI particles.

industrial price of the electricity, V is the total volume of treated solution (in m^3; four solutions were placed on the shaker at a time), and X is the mineralization efficiency of the process.

2.5. Experimental design strategy

For the AOPs, due to the multiplicity in the effect of operational parameters and their interactions, using statistical experimental design methods is vital [27]. The CCD is a popular five-level factorial design able to construct polynomial response surface models which has been introduced by Box and Wilson in 1951 [28]. It is composed of three points of the cube (related to the factorial design), axial, and center points. Hence, to model each process, the total run of the experiments (N) can be obtained by $N = 2^k + 2k + N_0$, where k is the number of the studied factors and the three terms are referred to the three mentioned points, respectively. The experimental error is calculated using the center point experiments and also the axial points distances from the center are dependent on the number of the studied factors [29].

In the work, the effective operating factors, including initial pH and initial dosages of PS and NZVI particle, were selected as the input variables. Also, the X and related DOC were simultaneously introduced into the experimental design matrix as the responses. Based on the CCD methodology of Design Expert Software, 20 tests under different operational conditions were performed. The range of variables and the designed tests accompany with the corresponding responses are presented in Table 2. The applied ranges for the variables were determined based on some preliminary experiments and the relevant experiences

Table 1
Industrial prices of the used chemicals and unit of the electricity [26]

	The chemicals					
Electricity	H_2SO_4 (98%)	NaOH	KPS (99%)	$NaBH_4$ (98%)	$FeSO_4{\cdot}7H_2O$ (98%)	Starch (99%)
0.0662 US$/kwh	0.4011 $/L	0.4 $/kg	1.47 $/kg	3.35 $/kg	0.11 $/kg	0.47 $/kg

Table 2
The range of variables, designed experiment matrix by the CCD methodology, and experimentally obtained responses

Variable	Range and level				
	$-\alpha$	−1	0	+1	$+\alpha$
A: pH	3.30	4.5	6.25	8.00	9.19
B: $[PS]_0$(mg L^{-1})	95.46	300.00	600.00	900.00	1,104.54
C: [NZVI] (mg L^{-1})	12.27	60.00	130.00	200.00	247.72

Designed experiment matrix

Runs	The variable factors			(*X*)		DOC (US$/$m^3$)	
	pH	$[PS]_0$ (mg L^{-1})	[NZVI] (mg L^{-1})	(Exp.)	(Pred.)	(Exp.)	(Pred.)
1	6.25	600	247.73	0.53	0.51	16.60	19.96
2	6.25	600	130	0.4	0.39	19.17	18.70
3	4.5	900	60	0.51	0.59	15.22	19.67
4	6.25	600	12.27	0.19	0.27	36.59	32.68
5	4.5	300	200	0.44	0.51	18.08	17.27
6	8	300	60	0.15	0.21	46.68	45.97
7	8	900	60	0.25	0.33	29.05	23.17
8	9.19	600	130	0.42	0.41	18.31	29.04
9	6.25	1,104.54	130	0.66	0.58	13.35	16.10
10	6.25	600	130	0.38	0.39	19.98	18.70
11	4.5	300	60	0.47	0.46	15.38	24.83
12	6.25	95.46	130	0.16	0.20	43.18	39.61
13	6.25	600	130	0.36	0.39	20.84	18.70
14	8	900	200	0.49	0.58	17.30	15.61
15	4.5	900	200	0.69	0.84	13.44	12.11
16	8	300	200	0.18	0.25	39.67	38.41
17	6.25	600	130	0.37	0.39	20.66	18.70
18	6.25	600	130	0.38	0.39	20.07	18.70
19	6.25	600	130	0.37	0.39	20.49	18.70
20	3.31	600	130	0.88	0.84	10.06	8.35

[30,31]. Also PS dosage range was selected considering allowable dose of sulfate in environments [32].

3. Results and discussion

Based on the obtained data from the performed experiments (Table 2), the following results are discussed.

3.1. The models establishment

The performed regression analysis by the software on the obtained data showed that the process responses can be simulated by the following second-order polynomial models as:

$$X = 1.71 - 0.41\,\mathrm{pH} + 5.11 \times 10^{-5}\,\mathrm{KPS} - 4.6 \times 10^{-4}\,\mathrm{NZVI} + 2.5 \times 10^{-6}\,\mathrm{KPS} \times \mathrm{NZVI} + 0.027\,\mathrm{pH}^2 \quad (14)$$

$$\mathrm{DOC} = 8.45 + 8.56\,\mathrm{pH} - 0.014\,\mathrm{KPS} - 0.196\,\mathrm{NZVI} - 8.38 \times 10^{-3}\,\mathrm{KPS} \times \mathrm{pH} + 3.65 \times 10^{-5}\,\mathrm{KPS}^2 + 5.5 \times 10^{-4}\,\mathrm{NZVI}^2 \quad (15)$$

where *X* and DOC (US$/$m^3$) are the mineralization efficiency and the demand-operating cost of the NZVI/PS process, respectively, and all of the terms are actual factors.

Variance analysis for the models was surveyed such that *p*-value less than 0.05 and greater than 0.10

indicate that the model terms are significant or not, respectively. The unsignificant terms in the models were omitted and the analysis of variance was done again for the obtained reduced quadratic models which results are shown in Tables 3 and 4, respectively. *F*-value and *p*-value of the models imply that they are significant and can predicte the responces satisfactorily. Linearity of the plots of actual data vs. predicted data in Fig. 3 approves the models can predict the efficiency of NZVI/PS process and its operating cost well.

3.2. Influence of the operating factors on the process responses

In order to survey the role of variables on the process characteristics, based on the established models, three-dimensional (3D) plots were prepared by the software. The response surface plot provides a visual option for prediction of the desired response at different amounts of the variables as well as it helps in identifying any influence of the variables interaction on the response [33]. In each plot, two factors are altered and another one is set at its zero level. Fig. 4(A) and (B) shows dependency of the efficiency and DOC vs. the initial pH and PS dosage, respectively.

The Fig. 4(A) shows that the process efficiency is increased at the acidic pHs and high dosages of the PS. In the presence of the higher PS concentration, more persulfate ions are available to produce the active PS radicals, hence the process efficiency is increased. At the alkaline pHs, dissolved iron ions are in the form of hydroxid and are less free in the media to react with PS ions. Also at this condition, the UDMH molecules are partly coagulated and cannot be exposed to the oxidation agent. So in alkline pH, the mineralization efficiency is low.

The process efficiency and DOC as a function of NZVI and PS dosage factors are shown in Fig. 5(A) and (B), respectively. The Fig. 5(A) shows that the efficiency is higher when both the factors are increased. But, the trend of *X*-variation with PS dosage is different at the low and high levels of the NZVI dosage as well as the trend vs. the NZVI variation is different at the low and high dosages of PS in the media. This means, each of the factors can exhibit the highest effect on the process only if the other is enough high. Based on Eq. (5), the active radicals are generated via interaction between the PS ions and ferrous ions, which are slowly produced by NZVI particles (Eqs. (7)–(9)) in the media. The figure shows that any restriction in the interaction can limit the process efficiency which is also confirmed by the ANOVA analysis (BC term in the Table 3). Also, the Fig. 5(B) demonstrates, as the NZVI and PS dosages are increased in the media, the DOC is deminished, due to the lower related EEC. It is notable that synergistic and antagonistic effect of each parameter on the process is in agrement with sign of the terms in Eqs. (14) and (15) such that positive signs indicate synergistic effect, whereas negative signs indicate antagonistic effect.

3.3. Optimization of the operating factors

The NZVI/PS process factors were optimized based on the two constructed models, while the main objects were to maximize the *X* and minimize the DOC by recalculating values of the factors using the desirability functions as a numerical facility of the software. The desirability (*D*) is an objective function that its value is in the range of 0–1, that the numerical optimization attains a maximum point of it. Also, before optimization, according to significance of the

Table 3
Analysis of variance for the reduced quadratic model belong to the mineralization efficiency

Source	Sum of squares	df	Mean square	*F*-value	*p*-value prob. > *F*
Model	0.607409	5	0.121482	31.4542	<0.0001
A-pH	0.240849	1	0.240849	62.36075	<0.0001
B-[PS]	0.173859	1	0.173859	45.01563	<0.0001
C-[NZVI]	0.072029	1	0.072029	18.64975	0.0007
BC	0.02205	1	0.02205	5.709206	0.0315
A^2	0.098623	1	0.098623	25.53567	0.0002
Residual	0.054071	14	0.003862		
Lack of fit	0.053137	9	0.005904	31.6293	0.0007
Pure error	0.000933	5	0.000187		
Cor total	0.66148	19			

Table 4
Analysis of variance the reduced quadratic model belong to the process cost

Source	Sum of squares	df	Mean square	*F*-value	*p*-value prob. > *F*
Model	1772.398	6	295.3997	11.57093	0.0001
A-pH	522.1948	1	522.1948	20.45458	0.0006
B-[PS]	660.3475	1	660.3475	25.86607	0.0002
C-[NZVI]	193.9219	1	193.9219	7.595996	0.0163
AB	154.7558	1	154.7558	6.061845	0.0286
B^2	156.8947	1	156.8947	6.145628	0.0277
C^2	105.5652	1	105.5652	4.13503	0.0629
Residual	331.8833	13	25.52948		
Lack of fit	330.0462	8	41.25577	112.285	<0.0001
Pure error	1.8371	5	0.36742		
Cor total	2104.282	19			

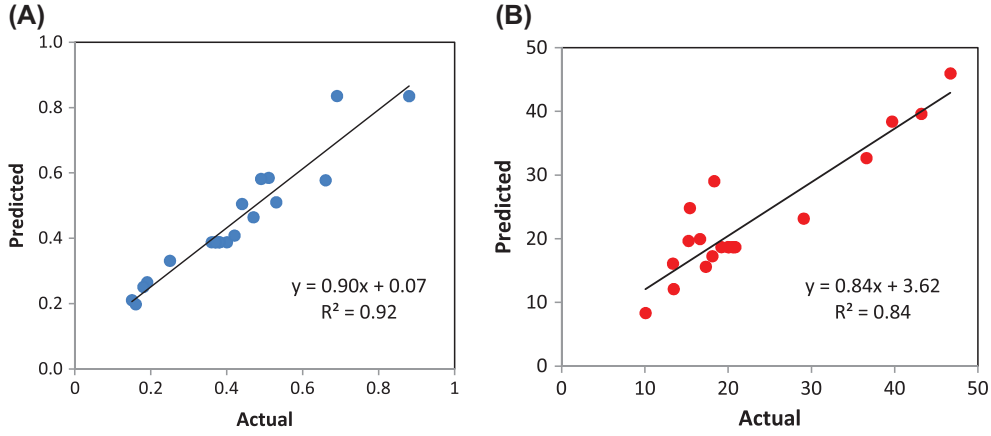

Fig. 3. Actual vs. predicted plots (A) mineralization and (B) process cost.

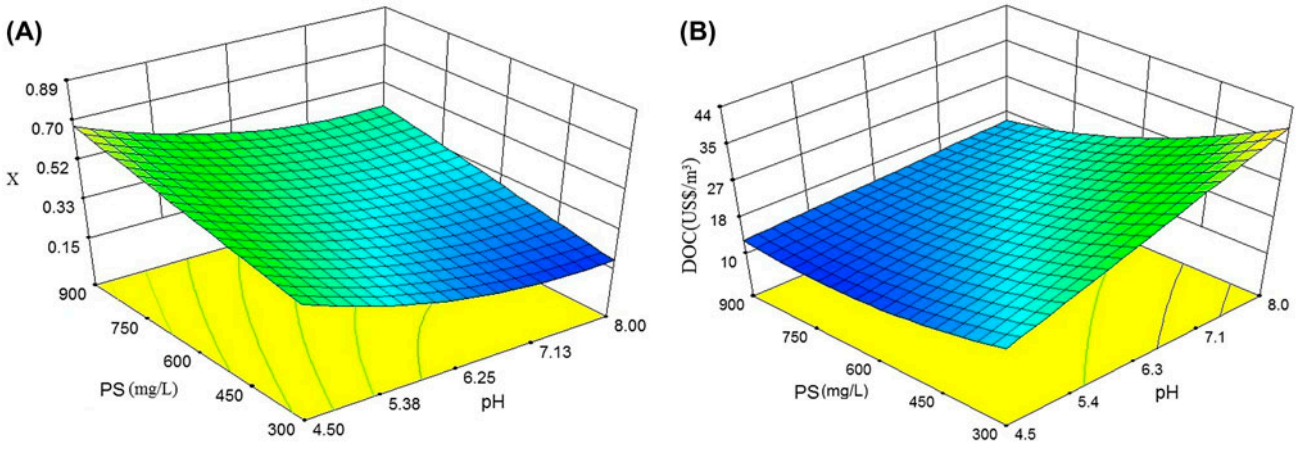

Fig. 4. Response surface plot of (A) the predicted X and (B) DOC vs. pH and PS dosage ($[UDMH]_0 = 50$ mg L^{-1}, and $T = 25$°C).

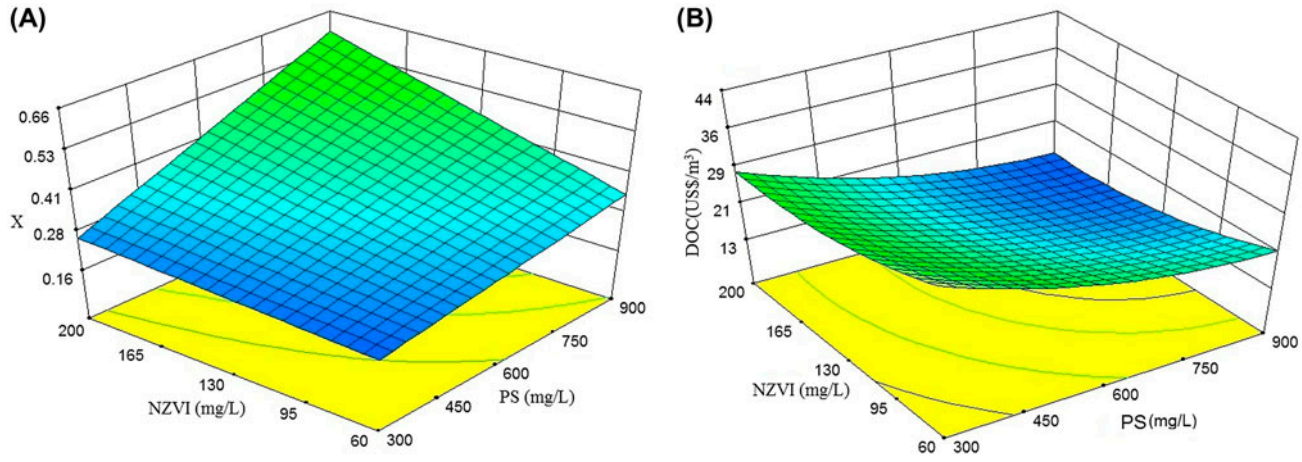

Fig. 5. Response surface plot of (A) the predicted X and (B) DOC vs. NZVI and PS dosages ($[UDMH]_0$ = 50 mg L^{-1}, and T = 25℃).

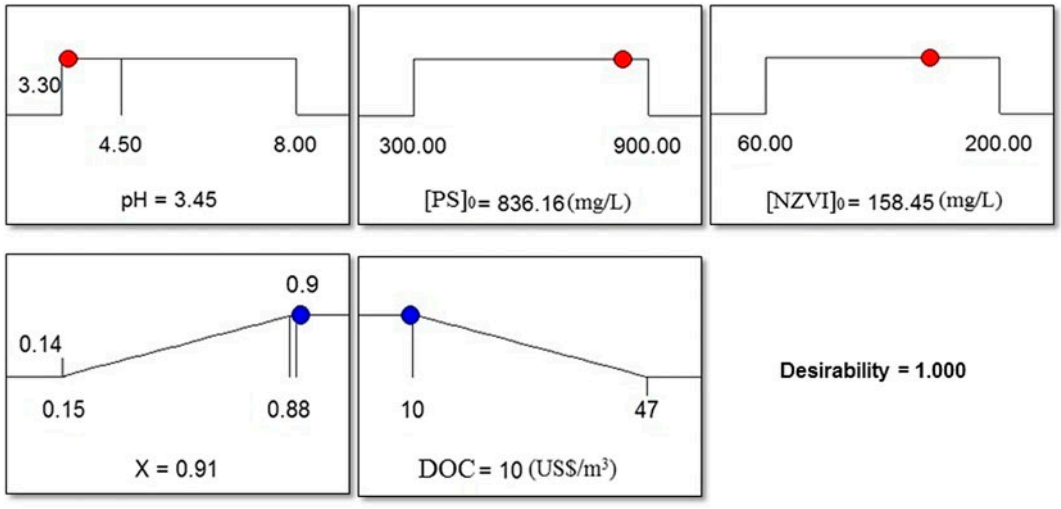

Fig. 6 The desirability ramp for the numerical optimization of the NZVI/PS process.

each applied factor, the importance of factor can be adjusted.

The following overall desirability function is used for several responses [34,35]:

$$D = (d_1^{v1} \times d_2^{v2} \times d_3^{v3}, \ldots, d_n^{vn})^{\frac{1}{n}}, \quad 0 \le v_i \le 1 (i = 1, 2, \ldots, n), \quad \sum_{i=1}^{n} v_i = 1 \tag{16}$$

where d_i indicates the response desirability (i = 1,2,3,...,n), n is the number of responses, and v_i represents the importance of responses that changes from 1 to 5. So, the overall desirability function D depends on the importance value.

In this work, the goal of the all operating factors were set "in the range" except of the pH which was set between 3.3 and 8 to ensure inhibition of the coagulation. Also, the desired goals for the X and DOC responses were set at maximum and minimum values, respectively, as well as their importance were adjusted in the levels of 5 and 4.

As it is illustrated by the Fig. 6, under the mentioned conditions, it was estimated to achieve 91% of the mineralization about 10 US$/$m^3$ is needed as the DOC under the optimum values of pH, initial dosages of the PS, and NZVI as 3.45, 836.16 (mg L^{-1}), and

Table 5
Comparison of the different UDMH oxidation processes

No	[UDMH]	Process	T (°C)	pH	Oxidizer	Efficiency	Refs.
1	1,185 (mg L^{-1})	Cu/H_2O_2	25	3–11	1,300 (mg L^{-1})	–	[36]
2	15,000 (mg L^{-1})	$M^{n+}/ads./O_2/H_2O_2$	25	7	13,600 (mg L^{-1})	–	[11]
3	5 (mg L^{-1})	HC/IAFP[a]	25	3	–	98.6% (Deg.)	[37]
4	600 (mg L^{-1})	$Fe/ZSM\text{-}5/H_2O_2$	25	2–7.4	34,000(mg L^{-1})	93% (Mine.)	[38]
5	50 (mg L^{-1})	NZVI/PS	25	3.45	836 (mg L^{-1})	91% (Mine.)	This work

[a]Hydrodynamic cavitation/Induced advanced fenton process.

158.45 (mg L^{-1}), respectively. It is notable that under the optimum condition, about 69% of the cost is related to the consumed electrical energy, hence further studies can focus on designing a more cost-effective process in this case.

3.4. Comparative review

Up to now, there is no considerable information about the removal of UDMH by oxidation process in the literatures, hence comparing the resuls of the previous researches [11,36–38] is useful. It is reported that generation of a potent carcinogen, i.e. N-nitrosodimethylamine (NDMA) is probable in the oxidation of UDMH [36]. When H_2O_2 is used as an oxidant, acidic pHs are suitable bacause production of the NDMA is more likely to be the case at basic pHs [36]. Also, oxidation by active species such as hydroxyl radicals can mineralize the UDMH and does not produce hazardous byproducts. The characteristics and results of this study accompany with the other literatures are presented in Table 5. The first, second, and third works in the table only are about oxidation of the UDMH and its mechanism, but not consider to the mineralization. The fourth case has reproted a good mineralization efficiency but it has used a great amount of oxidant ($[H_2O_{2in\ mmol}]/[UDMH_{in\ mmol}] = 100$). In the present work, this ratio is about 3.72 for 91% mineralization efficiency.

4. Conclusion

In the present study, a chemical method using NZVI particles was applied to active PS ions (named as NZVI/PS process) to mineralize the UDMH molecules as a hazardous matter in the aqueous media. Concisely, the related obtained information of the research can be listed as following:

(1) Based on the TEM analysis, the applied chemical precipitation method produced zero-valent iron particles with mean diameter size of 40 nm.
(2) The NZVI particles were successfully stabilized, before the application, using starch molecules as an eco-friendly stabilizer (confirmed by the DLS analysis).
(3) Two second-order polynomial equations were constructed by the CCD RSM to model the process efficiency and DOC as a function of applied effective factors.
(4) In the optimum conditions of pH 3.45, $[PS]_0$ = 836.16 mg L^{-1}, and $[NZVI]_0$ = 158.45 mg L^{-1}, the mineralization efficiency is equal to 91% with a DOC of 10 US$/$m^3$.
(5) Under the optimum conditions, about 69% of the operating cost is pertained to the consumed electrical energy, which reveals necessity of further studies to design more energy effective reactors.

References

[1] U.S. Environmental protection Agency, Health and Environmental Effects Profile for 1,1-Dimethylhydrazine EPA/600/X-84/134, Environmental Criteria and Assessment Office, Office of Research and Development, Cincinnati, OH, 1984.
[2] International Agency for Research on Cancer (IARC), IARC Monographs on the Evaluation of the Carcinogenic Risk of Chemicals to Man: Some Aromatic Amines, Hydrazine and Related Substances, N-Nitroso Compounds and Miscellaneous Alkylating Agents, World Health Organization, Lyon, 1974.
[3] K.G. Back, A.A. Thomas, Pharmacology and toxicology of 1,1-dimethylhydrazine (UDMH), Am. Ind. Hyg. Assoc. J. 24 (1963) 23–27.
[4] H.W. Schessl, K. Othmer, Ecyclopedia of Chemical Technology, fourteenth ed., Wiley/Interscience, New York, NY, 1995.
[5] M. Nauryzbaev, S. Batyrbekova, A. Razalne, G. Permenev, H. Vanoa, M. Turmukhanova, Contamination of soil, water and plants in Kazakhstan by components of rocket fuel because of rocket-related activity, Al-Farabi Kazakh National University, TRADE/WP.8/AC.1/SEM.7/2002/4/S.27.

[6] J. Saien, A.R. Soleymani, J.H. Sun, Parametric optimization of individual and hybridized AOPs of Fe^{2+}/H_2O_2 and $UV/S_2O_8^{2-}$ for rapid dye destruction in aqueous media, Desalination 279 (2011) 298–305.
[7] M.A. Al-Shamsi, N.R. Thomson, S.P. Forsey, Iron based bimetallic nanoparticles to activate peroxygens, Chem. Eng. J. 232 (2013) 555–563.
[8] D. Arapoglou, A. Vlyssides, C. Israilides, A. Zorpas, P. Karlis, Detoxification of methyl-parathion pesticide in aqueous solutions by electrochemical oxidation, J. Hazard. Mater. 98 (2003) 191–199.
[9] W.K. Jozwiak, M. Mitros, J. Kaluznaczaplinska, R. Tosik, Oxidative decomposition of Acid Brown 159 dye in aqueous solution by H_2O_2/Fe^{2+} and ozone with GC/MS analysis, Dyes Pigm. 74 (2007) 9–16.
[10] K. Ayoub, E.D. van Hullebusch, M. Cassir, A. Bermond, Application of advanced oxidation processes for TNT removal: A review, J. Hazard. Mater. 178 (2010) 10–28.
[11] O.P. Pestunova, G.L. Elizarova, Z.R. Ismagilov, M.A. Kerzhentsev, V.N. Parmon, Detoxication of water containing 1,1-dimethylhydrazine by catalytic oxidation with dioxygen and hydrogen peroxide over Cu- and Fe-containing catalysts, Catal. Today. 75 (2002) 219–225.
[12] R. Hazime, Q.H. Nguyen, C. Ferronato, T.K.X. Huynh, F. Jaber, J.M. Chovelon, Optimization of imazalil removal in the system $UV/TiO_2/K_2S_2O_8$ using a response surface methodology (RSM), Appl. Catal., B 132–133 (2013) 519–526.
[13] L. Dogliotti, E. Hayon, Flash photolysis of per[oxydi]-sulfate ions in aqueous solutions. The sulfate and ozonide radical anions, J. Phys. Chem. 71 (1967) 2511–2516.
[14] A. Tsitonaki, B. Petri, M. Crimi, H. Mosbæk, R.L. Siegrist, P.L. Bjerg, *In situ* chemical oxidation of contaminated soil and groundwater using persulfate: A review, Crit. Rev. Environ. Sci. Technol. 40 (2010) 55–91.
[15] I. Kolthoff, I. Miller, The Chemistry of persulfate. I. The kinetics and mechanism of the decomposition of the persulfate ion in aqueous medium 1, J. Am. Chem. Soc. 73 (1951) 3055–3059.
[16] C. Liang, C.J. Bruell, M.C. Marley, K.L. Sperry, Persulfate oxidation for *in situ* remediation of TCE. II. Activated by chelated ferrous ion, Chemosphere 55 (2004) 1225–1233.
[17] G.P. Anipsitakis, D.D. Dionysiou, Radical generation by the interaction of transition metals with common oxidants, Environ. Sci. Technol. 38 (2004) 3705–3712.
[18] G.V. Buxton, T.N. Malone, G. Arthur Salmon, Reaction of SO_4^- with Fe^{2+}, Mn^{2+} and Cu^{2+} in aqueous solution, J. Chem. Soc., Faraday Trans. 93 (1997) 2893–2897.
[19] C. Liang, Y.-Y. Guo, Mass transfer and chemical oxidation of naphthalene particles with zerovalent iron activated persulfate, Environ. Sci. Technol. 44 (2010) 8203–8208.
[20] D.H. Bremner, A.E. Burgess, D. Houllemare, K.-C. Namkung, Phenol degradation using hydroxyl radicals generated from zero-valent iron and hydrogen peroxide, Appl. Catal., B. 63 (2006) 15–19.
[21] Z. Xiong, D. Zhao, G. Pan, Rapid and complete destruction of perchlorate in water and ion-exchange brine using stabilized zero-valent iron nanoparticles, Water Res. 41 (2007) 3497–3505.
[22] L. Tielong, G. Bing, Z. Na, J. Zhaohui, Q. Xinhua, Hexavalent chromium removal from water using chitosan-Fe0 nanoparticles, in: 8th China International Nanoscience and Technology Symposium, J. Phys. Conf. Ser. 188 012057, IOP Publishing, 2009, doi: 10.1088/1742-6596/188/1/012057.
[23] W.Z.W. Yaacob, N. Kamaruzaman, A. Rahim, Development of nano-zero valent iron for the remediation of contaminated water, Chem. Eng. 28 (2012) 25–30.
[24] Ç. Üzüm, T. Shahwan, A. Eroğlu, I. Lieberwirth, T. Scott, K. Hallam, Application of zero-valent iron nanoparticles for the removal of aqueous Co^{2+} ions under various experimental conditions, Chem. Eng. J. 144 (2008) 213–220.
[25] J.B. Parsa, H.R. Vahidian, A. Soleymani, M. Abbasi, Removal of Acid Brown 14 in aqueous media by electrocoagulation: Optimization parameters and minimizing of energy consumption, Desalination 278 (2011) 295–302.
[26] Chemicals cost. Available from: <http://www.eia.gov, http://www.alibaba.com and http://www.made-in-china.com>, (Retrieved May, 20, 2014).
[27] J. Saien, A.R. Soleymani, H. Bayat, Modeling Fentonic advanced oxidation process decolorization of Direct Red 16 using artificial neural network technique, Desalin. Water Treat. 40 (2012) 174–182.
[28] G.E. Box, K. Wilson, On the experimental attainment of optimum conditions, J. R. Stat. Soc. Ser. B Stat. Method. 13 (1951) 1–45.
[29] D.C. Montgomery Design and Analysis of Experiments, Wiley, New York, NY, 1997.
[30] Y.G. Adewuyi, N.Y. Sakyi, Removal of nitric oxide by aqueous sodium persulfate simultaneously activated by temperature and fe^{2+} in a lab-scale bubble reactor, Ind. Eng. Chem. Res. 52 (2013) 14687–14697.
[31] A. Ghauch, G. Ayoub, S. Naim, Degradation of sulfamethoxazole by persulfate assisted micrometric Fe^0 in aqueous solution, Chem. Eng. J. 228 (2013) 1168–1181.
[32] D.R. Hitchcock, Biogenic contribution to atmospheric sulfate levels, in: Water's Interface with Energy, Air and Solids, Proceedings of the Second National Conference on Complete Water Reuse, Chicago, IL, 1975, pp. 291–310.
[33] Y.-J. Li, C.-C. Chang, T.-C. Wen, Application of statistical experimental strategies to H_2O_2 production on Au/graphite in alkaline solution, Ind. Eng. Chem. Res. 35 (1996) 4767–4771.
[34] V.A. Sakkas, M.A. Islam, C. Stalikas, T.A. Albanis, Photocatalytic degradation using design of experiments: A review and example of the Congo red degradation, J. Hazard. Mater. 175 (2010) 33–44.
[35] R. Lazic, Design of Experiments in Chemical Engineering: A Practical Guide, Wiley, Weinheim, 2004.
[36] G. Lunn, E.B. Sansone, Oxidation of 1,1-dimethylhydrazine (UDMH) in aqueous solution with air and hydrogen peroxide, Chemosphere 29 (1994) 1577–1590.
[37] M. Torabi Angaji, R. Ghiaee, Decontamination of unsymmetrical dimethylhydrazine waste water by hydrodynamic cavitation-induced advanced Fenton process, Ultrason. Sonochem. 23 (2015) 257–265.
[38] O.A. Makhotkina, E.V. Kuznetsova, S.V. Preis, Catalytic detoxification of 1,1-dimethylhydrazine aqueous solutions in heterogeneous Fenton system, Appl. Catal., B 68 (2006) 85–91.